ISSN: 2414-1895 DOI: 10.6919/ICJE.202405_10(5).0004

The Impact of SLM Process Parameters on the Mechanical Properties of IN718 Alloy

Yuanzheng Li

University of Shanghai for Science and Technology, Shanghai 200000, China

Abstract

The selective laser melting (SLM) process is utilized to fabricate IN718 alloy with scanning spacings of 0.04mm, 0.06mm, 0.08mm, and 0.1mm. The microstructure of the deposited and heat-treated alloys was examined using optical microscopy, Vickers microhardness testing, and electro-hydraulic servo high-speed tensile testing. The results demonstrate that SLM technology achieves excellent metallurgical bonding under varying process parameters. The microhardness of the alloy initially increases and then decreases with increasing scanning distance. Furthermore, the yield strength and elongation of the alloy increase as the scanning distance rises during high-speed tensile testing, indicating an enhancement in mechanical properties.

Keywords

Selective Laser Melting; IN718 Alloy; High Speed Drawing.

1. Introduction

IN718 alloy is a precipitation-strengthened nickel-based superalloy, which is widely used in aerospace and other fields because of its good high temperature corrosion resistance, corrosion resistance and excellent mechanical properties[1, 2]. The main strengthening element in IN718 alloy is Nb element, after aging treatment, the alloy will precipitate the strengthening phase γ "phase and γ 'phase at the grain boundary, and the precipitation of MC carbide and δ phase at the grain boundary, where the γ" phase has the same lattice as the matrix, and the lattice mismatch is very large, so it has a higher yield strength than the γ' phase in mechanics[3, 4]. Nb is not only the main forming element of the strengthened γ "phase and γ 'phase, but also the formed element of the strengthened δ phase and the brittle segregation phase Laves phase[5]. SLM technology is the use of high energy laser beam as a heat source for selective melting of alloy powder, combined with CAD/CAM and other technologies through the three-dimensional model into two-dimensional graphics, laser beam scanning according to the set path, from the point and line to the surface layer scanning, until the completion of the part forming[6].

Domestic and foreign scholars have also made relevant studies on the mechanical properties of IN718 alloy formed by SLM. Fang[7] et al. studied the structure and mechanical properties of IN718 alloy under different forming directions and angles of SLM, and the results showed that Nb and Mo elements have microscopic segregation, which can explain the formation of the strengthening phase. The mechanical properties after heat treatment are also higher than that of the deposited state. Hollond[8] et al. used electron diffraction experiment to observe and analyze the grain orientation of the heat treatment state and the deposition state of IN718 alloy formed by SLM. The results showed that the deposited alloy showed great anisotropy in grain morphology, and recrystallization of the alloy after heat treatment resulted in the formation of annealing twins, which also improved the mechanical properties. Schwarze [9]et al. studied the effect of solid solution treatment on the high temperature creep properties of IN718 alloy formed by SLM, and the results showed that a small amount of δ phase can improve the notch sensitivity and intergranular fatigue crack fracture resistance

ISSN: 2414-1895 DOI: 10.6919/ICJE.202405_10(5).0004

of the alloy. In this paper, the effects of different process parameters on mechanical properties of heat-treated alloys under high strain conditions are analyzed by high-speed tensile experiments.

2. Experiment

2.1 Experimental Materials and Experimental Processes

The powder used in the experiment was aero-atomized IN718 alloy powder, the main composition of which was shown in Table 1, and the particle size distribution of the powder was mainly 15μm-53μm. The high-speed tensile sample was formed using different process parameters. The forming process parameters were shown in Table 2, and the size of the high-speed tensile sample was shown in Figure 1. The heat treatment system used in the experiment was: 1050 ℃×1 h+ air cooling +720 ℃×8 h+50 ℃/h cooling for 2 h+620 ℃×8 h+ air cooling (HT1050). OPTI inverted metallography microscope (OM) was used to observe the microstructure of IN718 alloy in deposited and heat treated states. Using a Vickers hardness tester to test the hardness of the alloy, seven dot tests are performed on each test sample, and in order to reduce errors, the maximum and minimum values are removed and then the average value is taken. Instron electro-hydraulic servo high speed testing machine was used to carry out high speed tensile experiments, and the experimental tensile strain rate was 1×102.

Table 1. IN718 alloy powder main composition /%

Ni	Nb	Mo	Cr	Al	Ti	Co	C	P	Fe
52.93	5.08	3.04	19.10	0.48	0.84	0.01	0.042	0.0081	Bal.

Table 2. Forming process parameter setting

No.	Laser power/W	Scanning speed mm/s	Sweep spacing/mm
1	150	700	0.04
2	190	900	0.06
3	210	950	0.08
4	250	1100	0.10

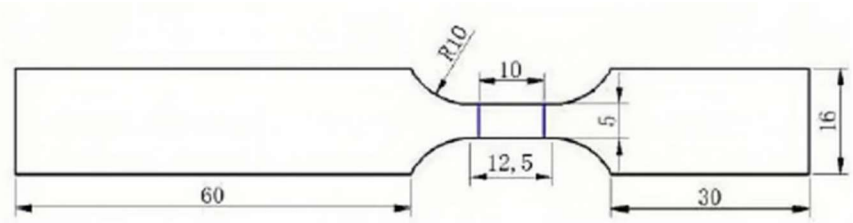

Figure 1. High speed tensile specimen size

3. Experimental Results and Analysis

3.1 Microstructure Analysis

Figure 2 shows the deposition state and heat treatment state after SLM forming IN718 alloy. By observing Figure 2 (a-b), it can be found that there are no obvious holes and cracks in the formed alloy sample, and the laser trace appears in the transverse section step by step, and the fish scale molten pool produced by the Gaussian[10] distribution of laser spot energy is obvious in the longitudinal section.The results show that the alloy achieves good metallurgical bonding during SLM forming. By observing the metallographic diagram of the heat-treated alloy in Figure 2 (c-d), it can be found that the molten pool appearance and morphology of the sample after heat treatment cannot be distinguished, indicating that almost complete recrystallization has occurred after heat treatment,

ISSN: 2414-1895 DOI: 10.6919/ICJE.202405_10(5).0004

and the grain distribution in the transverse section can be observed with alternating distribution of coarse and fine grains, which is because the laser scanning path exists in the SLM forming process. The lap part causes the alloy to remelt and the grain in the remelt zone to be refined[11].

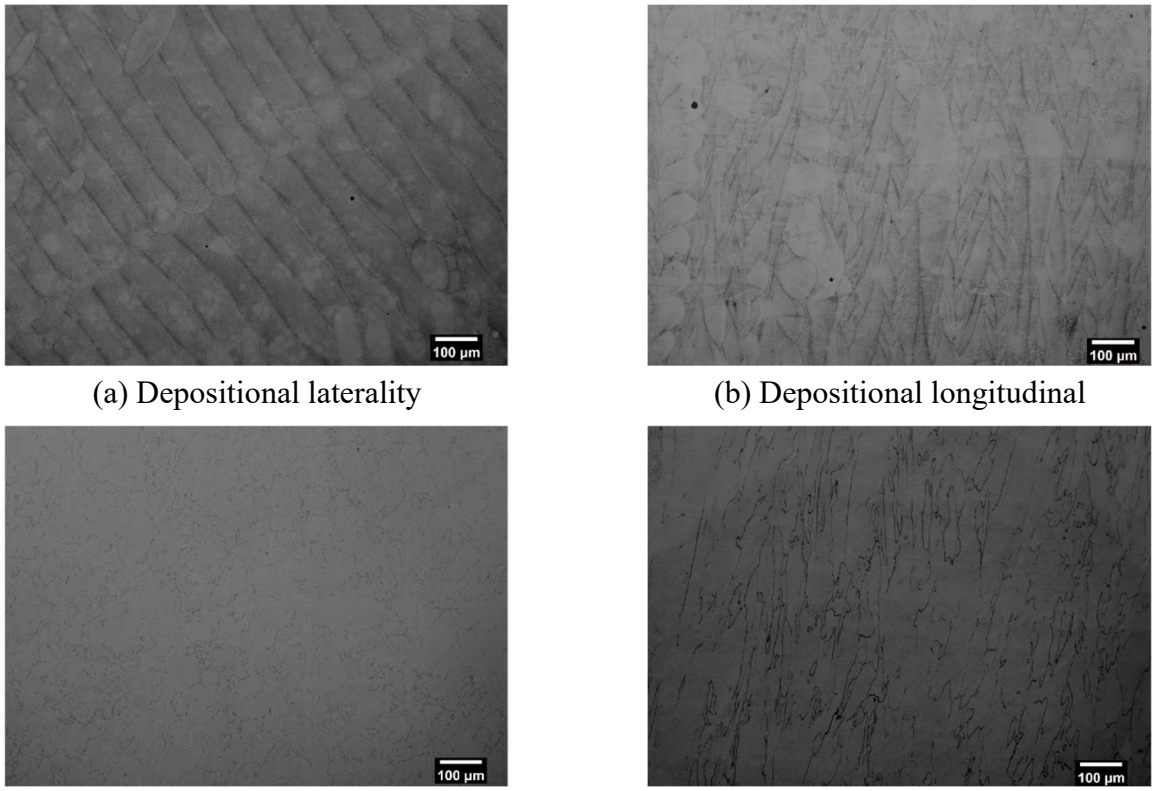

(a) Depositional laterality (b) Depositional longitudinal

(c) Transverse heat treatment (d) Longitudinal heat treatment

Figure 2. IN718 alloy deposited and heat treated metallography

3.2 Micro Vickers Hardness Analysis

Figure 3 shows the micro-Vickers hardness of the deposited and heat treated states under different parameters. The experimental results show that the lowest hardness of the deposited alloy is 284HV and the highest hardness is 299HV, while the lowest hardness of the heat treated alloy is 488HV and the highest hardness is 499HV.The hardness of the alloy after heat treatment is significantly higher than that of the deposited alloy, indicating that the grain remelting and recrystallization during the heat treatment process makes the grain fine, and the fine grain enhances the hardness of the alloy, because after the homogenization treatment at 1050℃ + double aging treatment, there is almost no carbonitride and brittle Laves phase in the organization. The segregation phenomenon of Nb element in the structure is greatly improved, and because more dispersion-distributed strengthening phase γ "phase and γ 'phase can be precipitated in the subsequent heat treatment process, and the alloy element can be more fully integrated into the austenite matrix at 1050℃, resulting in lattice distortion, which plays the role of solid solution strengthening, and greatly improves the hardness of the alloy[12]. It can also be seen from Figure 3 that with the increase of scanning spacing, the hardness of the alloy increases first and then decreases, because the size of scanning spacing determines the remelting zone between the fuse and the fuse. Too small scanning spacing will lead to too many remelting zones, which will make it easy to produce pores and other microscopic defects in the forming process, while too large scanning spacing will lead to a decrease in the remelting zone[13]. It will cause the alloy powder in some areas to melt insufficiently, resulting in unmelted particles and other defects, which will reduce the hardness of the alloy, so when the scanning spacing gradually increases, the hardness of the IN718 alloy will first increase and then decrease[14].

ISSN: 2414-1895 DOI: 10.6919/ICJE.202405_10(5).0004

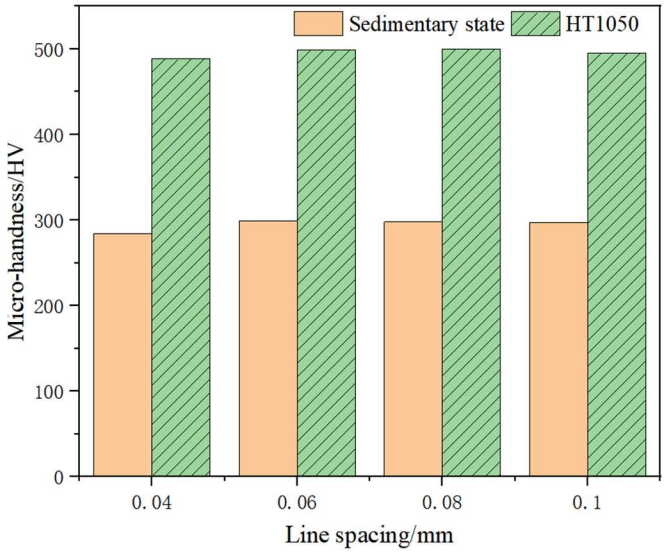

Figure 3. Hardness of IN718 alloy in different states

3.3 Analysis of High Speed Tensile Properties

Figure 4 shows the high-speed tensile stress-strain curve of IN718 alloy formed by SLM at 0.04mm, 0.06mm, 0.08mm and 0.1mm in heat treatment state. The results show that the tensile stress increases rapidly with the increase of strain at high strain rate, and begins to decline after reaching the maximum and finally breaks. The maximum tensile stress of the alloy increases with the increase of scanning spacing[15]. Figure 5 shows the high-speed tensile mechanical properties of IN718 alloy. The tensile strength and yield strength of the alloy at high strain rate gradually increase with the increase of scanning spacing, and the elongation after fracture first increases and then decreases with the increase of scanning spacing. The minimum tensile strength is 1425MPa, and the maximum tensile strength is 1624MPa. The increase of scanning spacing increases the tensile strength by 13.9%. The minimum yield strength is 1296MPa, and the maximum yield strength is 1460MPa. The increase of scanning spacing increases the yield strength by 12.6%. The minimum and maximum post-break elongation are 13.54% and 19.18%, respectively. The increase of scanning spacing increases the post-break elongation by 5.64%. The results show that the mechanical properties of IN718 alloy at high strain rate can be improved by increasing the scanning spacing in a proper range[16].

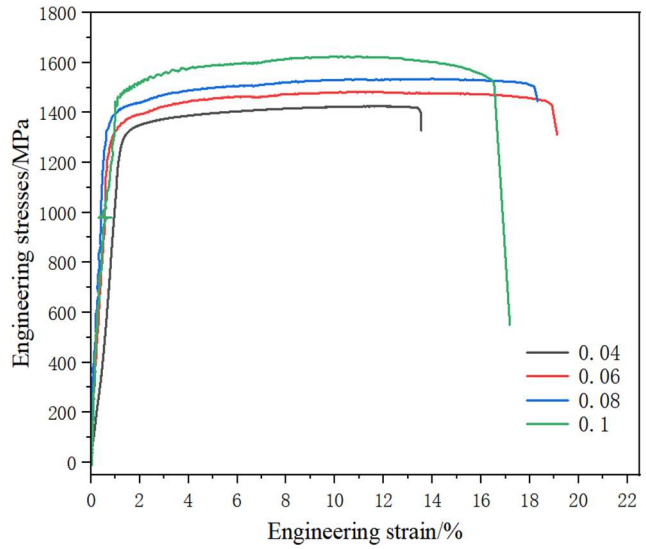

Figure 4. High speed tensile stress-strain curve of IN718 alloy

ISSN: 2414-1895 DOI: 10.6919/ICJE.202405_10(5).0004

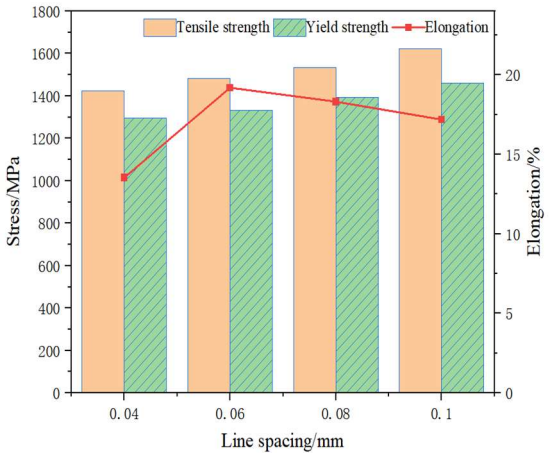

Figure 5. High speed tensile mechanical properties of IN718 alloy

Under the condition of high strain rate, the movement of dislocation is obviously intensified, the stress increase is more obvious, the shear stress increases and multiple slip systems can be activated at the same time, the dislocation density increases, and the dislocation entanglement phenomenon becomes more obvious, which also makes the high-speed tensile property higher than the normal tensile property[17].

4. Conclusion

(1) The IN718 alloy formed by SLM has good metallurgical bonding. Due to the influence of temperature gradient and cooling rate, the sedimentary structure is characterized by a columnar crystal structure growing along the epitaxial. After HT1050 heat treatment, the grain has a fine crystal zone, indicating that remelting and recrystallization occurred during the heat treatment process.

(2) The hardness of IN718 alloy in the heat treatment state is far greater than that of the deposited alloy. During the high heat treatment process, the alloying elements can be more fully integrated into the austenite matrix, resulting in lattice distortion, which plays a role of solid solution strengthening, and improves the hardness of the alloy. The hardness of the alloy also increases first and then decreases with the increase of the scanning distance.

(3) At the condition of high strain rate, the tensile strength and yield strength of IN718 alloy gradually increase with the increase of scanning spacing, and the elongation after fracture increases first and then decreases with the increase of scanning spacing. At the condition of high strain rate, the movement of alloy dislocation is obviously intensified, and the stress is obviously increased.

References

[1] MOHANTY S, SINGH MAURYA H, GOKULDOSS PRASHANTH K. Selective laser melting of Inconel 718: Effect of thermal treatment on mechanical properties [J]. Materials Today: Proceedings, 2023.

[2] MCLOUTH T D, WITKIN D B, BEAN G E, et al. Variations in ambient and elevated temperature mechanical behavior of IN718 manufactured by selective laser melting via process parameter control [J]. Materials Science and Engineering: A, 2020, 780: 139184.

[3] LU C, SHI J. Simultaneous consideration of relative density, energy consumption, and build time for selective laser melting of Inconel 718: A multi-objective optimization study on process parameter selection [J]. Journal of Cleaner Production, 2022, 369: 133284.

[4] JIA Q, GU D. Selective laser melting additive manufacturing of Inconel 718 superalloy parts: Densification, microstructure and properties [J]. Journal of Alloys and Compounds, 2014, 585: 713-21.

[5] GAO Y, ZHANG D, CAO M, et al. Effect of δ phase on high temperature mechanical performances of Inconel 718 fabricated with SLM process [J]. Materials Science and Engineering: A, 2019, 767: 138327.

ISSN: 2414-1895 DOI: 10.6919/ICJE.202405_10(5).0004

[6] FENG K-Y, LIU P, LI H-X, et al. Microstructure and phase transformation on the surface of Inconel 718 alloys fabricated by SLM under 1050°C solid solution + double ageing [J]. Vacuum, 2017, 145: 112-5.

[7] PENG J, LV X, LU Z, et al. Investigations of the mechanical and high-temperature tribological properties of the Inconel 718 alloy formed by selective laser melting [J]. Tribology International, 2023, 188: 108813.

[8] HOLLAND, SHARNIECE, WANG, et al. Grain boundary network evolution in Inconel 718 from selective laser melting to heat treatment [J]. Materials Science Engineering: A 2018.

[9] SCHWARZE, D., FREUND, et al. Superior creep strength of a nickel-based superalloy produced by selective laser melting [J]. Materials Science Engineering :A, 2016.

[10] SMITH D H, BICKNELL J, JORGENSEN L, et al. Microstructure and mechanical behavior of direct metal laser sintered Inconel alloy 718 [J]. Materials Characterization, 2016, 113: 1-9.

[11] WANG W, CHEN Z, LU W, et al. Heat treatment for selective laser melting of Inconel 718 alloy with simultaneously enhanced tensile strength and fatigue properties [J]. Journal of Alloys and Compounds, 2022, 913: 165171.

[12] ZHANG B, WANG P, CHEW Y, et al. Mechanical properties and microstructure evolution of selective laser melting Inconel 718 along building direction and sectional dimension [J]. Materials Science and Engineering: A, 2020, 794: 139941.

[13] ZHANG D, ZHANG P, LIU Z, et al. Thermofluid field of molten pool and its effects during selective laser melting (SLM) of Inconel 718 alloy [J]. Additive Manufacturing, 2018, 21: 567-78.

[14] ZHANG L, SHI X, LI N, et al. Heterogeneities of microstructure and mechanical properties for inconel 718 strut tensile sample fabricated by selective laser melting [J]. Journal of Materials Research and Technology, 2021, 12: 2396-406.

[15] RAGHAVAN S, ZHANG B, WANG P, et al. Effect of different heat treatments on the microstructure and mechanical properties in selective laser melted INCONEL 718 alloy [J]. Materials Manufacturing Processes, 2016: 10426914.2016.1257805.

[16] ZHAO Y, GUAN K, YANG Z, et al. The effect of subsequent heat treatment on the evolution behavior of second phase particles and mechanical properties of the Inconel 718 superalloy manufactured by selective laser melting [J]. Materials Science and Engineering: A, 2020, 794: 139931.

[17] HOLLAND, SHARNIECE, WANG, et al. Grain boundary network evolution in Inconel 718 from selective laser melting to heat treatment [J]. Materials Science Engineering, A, 2018.